Food Research International 162 (2022) 112073

Contents lists available at ScienceDirect

Food Research International

journal homepage: www.elsevier.com/locate/foodres

Bioactive compounds and enzymatic browning inhibition in cloudy apple juice by a new magnetic UVM-7-SH mesoporous material

Sara Muñoz-Pina [a], Aitana Duch-Calabuig [a], Elia Ruiz De Assín David [a], José V. Ros-Lis [b,*], Pedro Amorós [c], Ángel Argüelles [a,*], Ana Andrés [a]

[a] Instituto Universitario de Ingeniería de Alimentos para el Desarrollo (IUIAD-UPV), Universitat Politècnica de València Camino de Vera s/n, 46022 Valencia, Spain
[b] REDOLÍ, Departamento de Química Inorgánica, Universitat de València, 46100 Burjassot, Valencia, Spain
[c] Instituto de Ciencia de Materiales, Universitat de València, C/Catedrático José Beltrán 2, 46980 Paterna, Valencia, Spain

ARTICLE INFO

Keywords:
Magnetic UVM-7
Thiols
Enzymatic browning
Inhibition
Apple juice
Ascorbic acid
Total phenolics
Flavonoids
Flavonols
Antioxidant capacity

ABSTRACT

Fruits and vegetables juices present a high supply of polyphenols, making them highly exposed to enzymatic browning. In this work, we report a novel magnetized mesoporous silica material (Fe_3O_4NPs-UVM-7) functionalised with thiol and amine groups and evaluate their effect on the enzymatic browning as well as the physicochemical properties (pH and °Brix), bioactive compounds (ascorbic acid, total phenolics, flavonoids, and flavonols) and the antioxidant capacity of cloudy apple juice. From the obtained results, the mesoporous silica material magnetized by 11 % (w/w) with magnetite and functionalized with thiol groups reduce by 70 % the enzymatic browning in apple juice. It did not affect the physicochemical parameters such as pH or total soluble solids with respect to freshly squeezed juice. In addition, the content of flavonoids, vitamin C, and the antioxidant capacity measured by ABTS are also not affected by oxidation. However, the total content of polyphenols in the treated juice drops by 15 % compared to freshly squeezed juice, nonetheless, the loss is 20 % less than the control untreated. Thus, the material mitigates the loss of total polyphenols and also the antioxidant capacity.

1. Introduction

Fruits and vegetables include a wide and diverse group of plant foods whose energy and nutritional content varies remarkably between the different species (Slavin & Lloyd, 2012). Indeed, these types of food are known for their important concentrations of vitamins, minerals, and phytochemicals that function as antioxidants and anti-inflammatory agents (Bvenura & Sivakumar, 2017). Within this wide variety, apples (*Malus domestica*) are the second fruit most consumed in the European Union and the third most cultivated worldwide (87 million tons in 2019) (FAOSTAT, 2019).While a large portion of apples are consumed fresh (70 %), 25–30 % are converted into processed products, with apple juice concentrate as the main product (65 %). The rest is meant for value-added products including cider apple, apple puree and jams and dehydrated apple products among others (Cruz et al., 2018). Besides, apples are an important source of phenolic compounds, including flavonoids (such as flavonols and flavanols) (Kaushal, Singh, & Singh-Sangwan, 2022) and phenolic acids (such as chlorogenic acid, gallic acid, and caffeic acid) (Kalinowska, Bielawska, Lewandowska-Siwkiewicz, Priebe, & Lewandowski, 2014; Massini, Rico, & Martin-Diana, 2018). Traditionally, apple juice has been commonly consumed as clear juice, unfortunately, the clarification process implies the loss of about 50–90 % of these compounds (Kolniak-Ostek, Oszmiański, & Wojdyło, 2013). The growing tendency to consume fresher and minimally processed foods has increased sales of cloudy juices with a much higher concentration of polyphenols (Marszałek et al., 2018). Nevertheless, the elevated amounts of these bioactive compounds make them highly susceptible to enzymatic browning and a problem for the industry to assure colour stability (Kolniak-Ostek et al., 2013).

The browning of cloudy apple juices is mainly due to the polyphenol oxidase enzyme (PPO) (Illera et al., 2019). PPO compromises diverse copper-containing enzymes (catechol oxidase (EC 1.10.3.1), tyrosinase (EC 1.14.18.1), and laccase (E.C. 1.10.3.2)), and is wildly distributed in nature: animals, plants, and fungi (Kanteev, Goldfeder, & Fishman, 2015). Depending on the nature of the PPO, this enzyme can catalyse two different reactions. In the first place, the hydroxylation of monophenols to *o*-phenols, and in the second place, the oxidation of the *o*-phenols into quinones. Quinones are very reactive compounds that

* Corresponding authors.
E-mail addresses: J.Vicente.Ros@uv.es (J.V. Ros-Lis), anarfoi@tal.upv.es (Á. Argüelles).

https://doi.org/10.1016/j.foodres.2022.112073
Received 22 June 2022; Received in revised form 14 September 2022; Accepted 18 October 2022
Available online 21 October 2022

polymerise with other quinones, amino acids, or proteins generating reddish-brownish pigments called melanonids, which are the reason for colour change (Jukanti, 2017). This process, known as enzymatic browning, is not unique to apples but is the main cause of colour change in fruits and vegetables. Since the main factors that enhance the PPO activity and therefore the enzymatic browning are the concentration of polyphenols and the active enzyme, fruits and vegetables are the most affected foods. This reaction starts when there is a cell disruption in the matrix and PPO, polyphenols, and oxygen meet (Singh, Suri, Shevkani, Kaur, Kaur, & Singh, 2018). This tissue damage usually happens during harvesting, handling, and post-harvest processing like in the juice industry.

The colour change caused by enzymatic browning can cause consumer rejection, leading to food waste and economic losses (Raak, Symmank, Zahn, Aschemann-Witzel, & Rohm, 2017). To minimize the problem, the food industry has adopted different methodologies to prevent enzymatic browning. Thermal pasteurization has been the gold standard to prevent both enzymatic browning and destroying microorganisms (Ali, Popović, Koutchma, Warriner, & Zhu, 2020). However, applying temperatures between 60 and 90 °C results in undesirable sensorial and nutritional changes due to the damage of volatile and thermosensitive compounds (Sauceda-Gálvez et al., 2021). Other no-thermal treatments have been developed over the years to replace pasteurization. Ultrasounds, CO_2 supercritical, ultrafiltration, ultraviolet radiation, high-pressure homogenization or high hydrostatic pressure are some of the alternatives (Putnik et al., 2019). However, even though most of these techniques can be satisfactory, their effect can vary depending on the process parameters used and product characteristics (Cappato et al., 2017; Kruszewski, Zawada, & Karpiński, 2021). Besides, some negative effects on food properties, insufficient enzyme inactivation or the high cost have restricted their implementation (dos Santos Aguilar, Cristianini, & Sato, 2018; Muñoz-Pina, Ros-Lis, Argüelles, & Andrés, 2019).

In recent years, the implementation of nanotechnology in the food industry has had a prominent growth with good results (Ameta, Rai, Hiran, Ameta, & Ameta, 2020; Hamad, Han, Kim, & Rather, 2018). However, these studies have been focused mainly on encapsulation and packaging, but not on industrial processes (Pérez-Esteve, Bernardos, Martinez-Manez, Barat, & J., 2013). Thus, in order to find a new solution to this challenge, our working group has proved the use of silica mesoporous nanomaterials as candidates for PPO inhibition. UVM-7 material is a mesoporous material that was synthesized for the first time at the University of Valencia in 2002, based on the "atrane route", and given the name of UVM-7 (University of Valencia Material n°7) (El Haskouri et al., 2002). This material is characterized by having both intra-particle and interparticle pores, which provide the material with a large surface area and a stable pore distribution. These features make these supports ideal for hosting and interacting with enzymes. The material UVM-7 functionalised with thiol groups, was able to both immobilise and inhibit polyphenol oxidase in model systems and to stop the enzymatic browning in apple juice (Muñoz-Pina et al., 2018). Besides, in another recent publication (Muñoz-Pina, Ros-Lis, Argüelles, Martínez-Máñez, & Andrés, 2020), the material UVM-7 was functionalised with amine groups and it was proved that the material was capable of capturing not only the PPO but also the oxidation products.

However, the main drawback was the need for filtration to remove the material losing most of the bioactive compounds present in the juice (Rascon Escajeda et al., 2018). Moreover, even proved their effectiveness against the PPO, no studies were made of their influence on the other important quality parameters of apple juice that could meet the demands of consumers as well. Therefore, the main objective of the present study is to develop a new magnetic UVM-7 mesoporous silica material removable from the juice functionalised with thiol and amine groups. Besides, it was evaluated their effect on physicochemical (pH, °Brix, colour formation), bioactive compounds (ascorbic acid, total phenolics, flavonoids and flavonols) and the antioxidant capacity of cloudy apple juice.

2. Materials and methods

2.1. Chemicals

Tetraethyl orthosilicate (TEOS) reagent grade 98 %, triethanolamine (TEAH3) reagent grade 98 %, N- cetyltrimethylammonium bromide (CTABr) for molecular biology ≥99 %, 3-aminopropyl triethoxysilane (APTES) ≥98 %, 3-mercaptopropyl trimethoxysilane 95 %, sodium nitrite reagent grade 97 %, 6-Hydroxy-2,5,7,8-tetramethylchromane-2-carboxylic acid (Trolox 97 %), 2,2-Diphenyl-1-picrylhydrazyl (DPPH), gallic acid (97.5–102 % titration), L-Ascorbic acid >99 %, 2,4,6-Tris(2-pyridyl)-s-triazine (TPTZ 98 %), Quercetin >95 %, chloroform >99 %, (+)-Catechin hydrate 98 %, 1,2-dihydroxybenzene >99 %, sodium oxalate >99.5 %, ammonia solution 32 % and oleic acid 99 % were provided by Sigma-Aldrich (Sigma-Aldrich, USA). Sodium carbonate anhydrous, potassium dihydrogen phosphate, sodium bisphosphate, disodium phosphate and were acquired from Scharlau at reagent grade (>99 %) (Sharlab S.L., Spain). Sodium acetate, iron (III) chloride hexahydrate 97 %, iron (II) chloride tetrahydrate 97 %, methanol 99.9 %, Folin- Ciocalteu reagent, potassium persulfate >99 % and aluminium chloride >99.0 % were purchase from Honeywell (Honeywell, France). Finally, sodium hydroxide 1N standard volumetric solution came from Panreac AppliChem (Panreac AppliChem, Barcelona, Spain) and 2,2′-Azino-bis(3-ethylbenzthiazoline-6-sulfonic acid (ABTS) from Roche® Life Science Products.

Golden Delicious apples obtained in a local store were used to obtain the fresh juices used in the tests.

2.2. Synthesis of the magnetic UVM-7

Magnetic UVM-7 (Fe_3O_4NPs-UVM-7) was prepared following a two-step procedure. In a first step, small superparamagnetic iron oxide nanoparticles were synthesized following the method presented by Sánchez-Cabezas, Montes-Robles, Gallo, Sancenón, and Martínez-Máñez (2019) (Sánchez-Cabezas et al., 2019). Briefly, under a nitrogen atmosphere, 50 mL of distilled water were heated at 80 °C followed by the addition of 12 g of $FeCl_3{\cdot}6H_2O$ and 4.9 g of $FeCl_2{\cdot}4H_2O$. Then, 19.53 mL of ammonia 32 % was added and the mixture was left under stirring for 30 min. Subsequently, 2.13 mL of oleic acid was included in the mixture and kept under stirring for another 90 min at 80 °C. Once the mixture was cool down to room temperature, the blend was centrifuged at 12100*g* for 10 min. The precipitate was washed three times with distilled water and three more times with ethanol. The resulting magnetic black material was dried under vacuum overnight and resuspended in chloroform to avoid oxidation, forming a ferrofluid. In order to discard the largest nanoparticles and adjust the size of the final nanoparticles, the ferrofluid was centrifuged at 13400*g* for 20 min.

The water-Fe_3O_4NPs mixture was prepared previously with a phase-transfer of the ferrofluid to water (Sánchez-Cabezas et al., 2019). First, 1.6 g of CTAB were dissolved in the 80 mL of distilled water, followed by the addition of 16 mL of the Fe_3O_4NPs suspended in chloroform (6.5 mg/mL). Then the two-phase solution was micro-emulsified using a probe sonicator (Sonics Vibra cell VCX130; Sonics & Materials Inc., USA) with 2-second pulses and 100 % amplitude for 2 min using a 13 mm Tip diameter probe. Finally, the emulsion was heated at 65 °C under constant stirring until chloroform was evaporated entirely, giving a clear suspension of nanoparticles in water.

Once the small iron oxide nanoparticles (Fe_3O_4NPs) in the form of magnetite were synthesised, we proceeded to its coating with silica forming the UVM-7. A traditional UVM-7 synthesis with modification was followed. A mixture of TEOS (0.05 mol) and $TEAH_3$ (0.17 mol) was heated to 140 °C until no condensation of ethanol was observed. The reaction was cooled to 90 °C and 2.96 g of CTAB was gradually added followed by 80 mL of the water- Fe_3O_4NPs mixture. The blend was aged

at room temperature for 16 h and the resulting precipitate was collected by centrifugation (10000 × g) and washed with water and ethanol. Lastly, the final magnetic silica UVM-7 was dried at 40 °C and calcined in an oxidant atmosphere at 550 °C for 5 h. The functionalisation with the thiol (-SH) and amine (–NH_2) groups were carried out following known procedures (Muñoz-Pina, Amorós, Haskouri, Andrés, & Ros-Lis, 2020; Muñoz-Pina et al., 2018).

2.3. Material characterization

X-ray diffraction (PXRD) was measured in a Bruker AXS D8 Advance diffractometer using CuKα radiation and working at 40 kV/40 mA. Nanoparticles size distribution was studied by dynamic light scattering (DLS) using a Malvern Zetasizer Nano-ZS equipment working at 25 °C. Transmission electron microscopy (TEM) images were recorded using a JEOL JEM-1010. Specific surface area, pore size distribution, and pore volume were measured from nitrogen adsorption-desorption isotherms in a Micromeritics ASAP 2020 instrument. Si/Fe molar ratio (wt %) was determined with the EDX-Philips SEM-515 equipment. Thermal Gravimetric Analysis (TGA) in a TGA 550 Discovery from TA instruments was used to quantify the content of thiol and amine groups.

2.4. Cloudy apple juice preparation and polyphenol oxidase (PPO) activity determination

Golden Delicious apples were first washed and then the juice was prepared using a juicer (Moulinex centrifugal JU200045). The cloudy apple juice was analysed immediately after preparation. Polyphenol oxidase from the cloudy apple juice was determined following known procedures (Illera et al., 2019). Briefly, 100 μL of the apple juice was mixed with 2.9 mL of catechol solution (0.05 M) previously prepared in a 0.1 M phosphate buffer at pH 6.5. The oxidation reaction was followed spectrophotometrically (UV/vis, Beckman Coulter du 730), measuring the absorbance increase at 420 nm during 120 s. The PPO activity was taken as the slope of the linear stretch of the reaction curve. To determine the maximum PPO enzyme activity, the activity was measured at different times after making the juice (0, 5, 10, 20, and 30 min).

The best ratio material/[PPO] was determined by analysing the PPO activity in the presence (without removing the material from the juice) of the Fe_3O_4NP-UVM-7 functionalised and non-functionalised. For this, 15 mg of the material was mixed with 1 mL of three apple juice dilutions (1, ½, and ¼). The mixture was kept under stirring for 10 min and subsequently the same enzymatic assay was accomplished. Control without the material was also carried out. The assays were done in triplicate at 20 °C.

2.5. Fe_3O_4NP-UVM-7 treatment

Once the best ratio material/[PPO] was selected, the effect of the material on the physico-chemical characteristics of the juice was analyzed. For that, an aliquot of 2 mL of apple juice was mixed with the three different materials in concertation of 15 mg/mL (Fe_3O_4NPs-UVM-7, Fe_3O_4NPs-UVM-7-SH, and Fe_3O_4NPs-UVM-7-NH_2) in a 10 mL-glass vial using a magnetic stir plate at 600 rpm (IKA RTC Basic, Germany) for 10 min. Afterwards, the material was removed by a neodymium magnet and the sample was kept under stirring for 30 min more. For the different tests explained below, the needed aliquots were taken before removing the material, just after taking off the material and after 30 min with no material present. Measurements were performed in triplicate in three independent vials. A sample without material was used as a control.. Besides, a blank with the inhibitors was also measured and subtracted if present. The repetitions of the treatment were experimented by triplicate, three different vials, and from each vial the samples were made in duplicate.

2.5.1. Determination of total soluble solids (°Brix) and pH

The pH of the juices was determined using a digital pH meter (Metler Toledo SevenEasy. Total soluble solids (TSS) were determined using a digital refractometer (Atago-3 T) at 20 ± 1 °C and results were expressed in the standard °Brix unit.

2.5.2. Inhibitory effect of enzymatic browning

The oxidation process and the colour change were measured to assess the inhibitory effect by using a spectrophotometer Minolta (CM-3600 d). CIE L*a*b* (CIELAB) colour space which comprises L* (lightness), a* (red to green) and b* (yellow to blue) coordinates were obtained using a D65 illuminant and 10° observer as a reference system. The total colour difference (ΔE*) between the juice at time 0 and treated samples was calculated following the equation (1).

$$\Delta E^* = \sqrt{(\Delta L^*)^2 + (\Delta a^*)^2 + (\Delta b^*)^2} \quad (1)$$

2.5.3. Determination of total phenolic content (TPC) and antioxidant activities.

Total phenolic content (TPC) of juices were performed according to the Folin-Ciocalteu method (Aranibar et al., 2018). A mixture of 10 μL aliquot of the apple juice, 1.58 mL of deionized water, and 100 μL of the Folin-Ciocalteu reagent was left for 3 min. Afterwards, 300 μL of Na_2CO_3 (20 % w/v) was added and left in dark for 60 min before measuring the absorbance at 765 nm (UV/vis, Beckman Coulter du 730). A standard curve of gallic acid from 0 to 500 mg/L was prepared ($r^2 = 0.997$) and the results were reported as mg of gallic acid equivalent (GAE) (mg GAE/L).

For the antioxidant activities analysis, three different methods were conducted. One assay used to assess the antioxidant capacity was the ferric reducing antioxidant power assay (FRAP) following the method described by Thaipong, Boonprakob, Crosby, Cisneros-Zevallos, and Hawkins Byrne (2006) (Thaipong et al., 2006). In brief, an aliquot of 25 μL of the juices was reacted with 2850 μL of FRAP solution and 125 μL of distilled water for 30 min in dark condition. Then the absorbance was measured at 593 nm in a UV/vis, Beckman Coulter du 730. FRAP reagent was prepared by mixing in a ratio 10:1:1 a solution of 300 mM acetate buffer (pH 3.6), 20 mM ferric chloride and 10 mM TPTZ in 40 mM HCl. A standard curve of Trolox was set ($r^2 = 0.999$) and the results were stated as mg of Trolox equivalent per L (mg Trolox/L).

The antioxidant activity of the treated and untreated juices was also studied by DPPH· method investigating their ability to scavenge the $DPPH^●$ free radical (Wu et al., 2020) with slight modifications. A sample of 10 μL of juice was added to 1 mL of methanolic solution of $DPPH^●$ (100 μM). Then, the mixture was kept in the dark for 30 min and absorbance was measured at 517 nm using UV/vis spectrophotometer. The data were expressed as Trolox equivalent (mg Trolox/L) after getting the corresponding calibration curve ($r^2 = 0.990$).

Finally, the capacity to scavenge the $ABTS^{●+}$ free radical was tested by the established $ABTS^{●+}$ assay (Thaipong et al., 2006). A 1:1 solution of 7.4 mM $ABTS^{●+}$ solution and 2.6 mM potassium persulfate solution was prepared and left in the dark to react for 12 h at room temperature. Then, 1 mL of the solution was diluted in 60 mL of methanol. For the assay, 10 μL of the apple juice was mixed with 140 μL of distilled water and 2890 μL of the $ABTS^{●+}$ for 2 h in dark conditions. Then the absorbance was taken at 734 nm in the same spectrophotometer. The data were expressed as Trolox equivalent (mg Trolox/L) after getting the corresponding calibration curve ($r^2 = 0.997$).

2.5.4. Determination of total flavonoids and flavonols

The total content of flavonoids and flavonols was estimated following the methodology published by Abid et al. (2013) (Abid et al., 2013). For flavonoids, 100 μL aliquot of juice sample was mixed with 1.4 mL of deionized water and 75 μL of a 5 % $NaNO_2$. Afterwards, the sample was left for 6 min and 150 μL of a 10 % $AlCl_3$ was included and

then after 5 min, 0.50 mL of 1 M NaOH was added. Finally, the absorbance was measured at 510 nm previous to a calibration curve of (+)-catechin ($r^2 = 0.993$). The results were reported as mg of catechin equivalent/L.

For the total flavonols content, a 0.1 mL of juice was diluted with 0.4 mL of distilled water and mixed with 0.5 mL of 2 % $AlCl_3$ solution, followed by the addition of 0.5 mL sodium acetate solution (50 g/L). The mixture was left for 150 min at 20 °C, and then, the absorbance was read at 440 nm. A standard curve of quercetin from 0 to 150 mg/L was prepared ($r^2 = 0.998$) and the results were reported as mg of quercetin equivalent/L.

2.5.5. Determination of ascorbic acid

The content of ascorbic acid was measured according to the method reported by Selimović, Salkić, & Selimović, 2011 (Selimović et al., 2011). A sample of 50 μL was mixed with 1.95 mL of 1.13 mM of sodium oxalate dissolved in a potassium dihydrogenphosphate (30 mM)/ disodium hydrogenphosphate (0.8 mM) buffer solution (pH = 5.4). Subsequently, the absorbance was measured at 266 nm and data was confronted to a standard curve of L-ascorbic acid ($r^2 = 0.999$).

2.6. Software and data analysis

Data are reported as mean ± standard deviation. Statgraphics Centurion XVII software was used to perform the analysis of variance (One-Way ANOVA) and Multiple Range Tests by the LSD procedure (least significant difference) of the Fisher test to identify homogeneous groups. Besides, data were subjected to a Pearson correlation analysis to find the linear relationship between variables. A confidence level of 95 % (p-value < 0.05) was used in all cases.

3. Results and discussion

3.1. Description of Fe_3O_4NP-UVM-7

UVM-7 mesoporous silica particles functionalised with thiol and amine groups have shown their potential to avoid or delay the enzymatic browning when the material was removed (Muñoz-Pina et al., 2018, Muñoz-Pina et al., 2020). However, juice filtration leads to the loss of most of its bioactive compounds. To solve this issue, a new UVM-7 magnetic material that allows us to remove it from the medium without filtering the juice was herein developed and functionalised with thiol (-SH) and amine ($-NH_2$) groups.

To synthesise the new Fe_3O_4NPs-UVM-7, a two-steps route was designed. In the first place, it was necessary to develop small magnetic nanoparticles that were able to be introduced into the UVM-7 without breaking its morphology. PXRD powder diffraction and DLS were used to characterize the nanoparticles. The XRD pattern (Fig. 1A) shows that the final Fe_3O_4NPs correspond to crystalline magnetite (Fe_3O_4) presenting well-defined diffraction peaks at 2θ values of 30.17, 35.46, 43.09, 53.28, 56.88, and 62.45 (in good agreement with the JCPDS file no. 19-0629). Furthermore, the relative intensities of the peaks agree with the Bragg reflections of magnetite which were indexed as the crystallography planes (220), (311), (400), (422), (511) and (440). By applying the Scherrer equation (Patterson, 1939) for the determination of the crystallite size a value of 12.4 nm is obtained, which is in good correlation with the dimensions previously determined through TEM (irregularly shaped crystals, with sizes ranging from 4 to 26 nm and an average size of 10.3 ± 3.80 nm) (Sánchez-Cabezas et al., 2019). On the other hand, the size distribution of the nanoparticles was measured using dynamic light scattering (DLS) with a particle size of 20 nm. Hydrodynamic diameters are often overestimated compared to those observed by TEM (Yamada et al., 2012) due to the presence of a hydration shell and the stronger response of larger particles (Schoeman, Sterte, & Otterstedt, 1995). This overestimation may be even greater when compared to the determined particle sizes by XRD because a particle can be formed by several crystallites. Therefore, the differences observed are expected and consistent with the peculiarities of each technique. Once the magnetite was synthesised, it proceeded to the synthesis of the Fe_3O_4NPs-UVM-7. For this, different Magnetite/Si ratios (1, 2, and 3 g magnetite/mol TEOS) were tested during the synthesis of the particles. Small ratios generated slightly magnetic UVM-7 which only 4.6 ± 0.4 % wt of Fe at the final particles measured with EDX. On the other hand, large ratios caused a disruption of the UVM-7 in which its textural pore disappears (textural pore volume = 0.13 cm^3/g; textural pore diameter = 20 nm).

Nevertheless, an optimum Magnetite/Si ratio during the synthesis (2 g magnetite/mol TEOS) was found, where the Fe_3O_4NPs-UVM-7 solid was magnetic enough to remove it from a solution by appliying a Nd magnet (11 % wt of Fe in the final particle). The XRD pattern of the silica at the low-angle regime shows an intense peak and a shoulder at 2θ values around 2° and 4° that can be indexed to the (100) and the overlapped (110) and (200) reticular planes, respectively (assuming a hexagonal cell). (Fig. 1B). This confirms the preservation of the typical UVM-7 mesostructure (and the mesoporosity after the template removal). As seen in Table 1, d100 spacing calculated from the PXRD data was around 40 Å which coincides with other reported values (Haskouri et al., 2009). In addition, the XRD pattern recorded at high-angles (Fig. 1A) clearly shows the presence of low intensity peaks at 2θ values matching with the signals observed for the starting magnetite nanocrystals. The relatively low intensity of these peaks is due to the low Fe content. In addition, the TEM images (Fig. 1C and Figure S1) show the typical structure of the UVM-7 inorganic matrix in which small black spots scattered throughout the material can be observed in relation to the magnetite nanoparticles. An image with higher magnification is shown in the inset of Fig. 1C, showing a representative magnetite

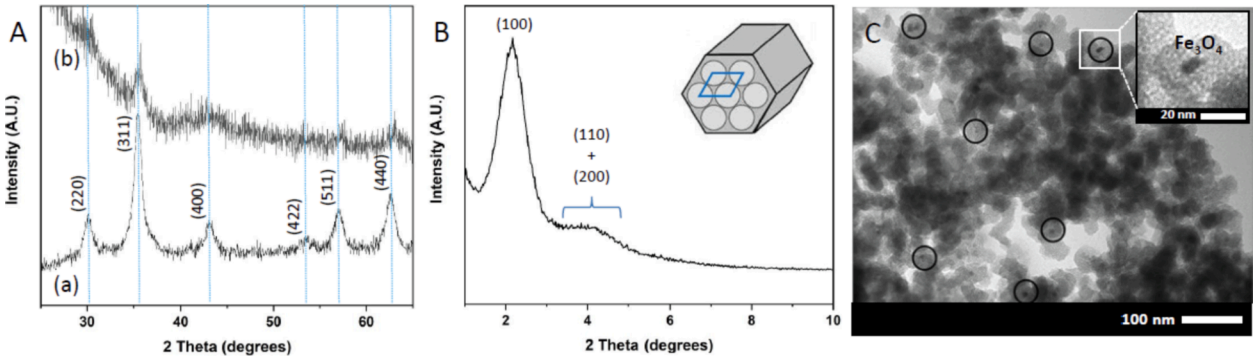

Fig. 1. (A) High-angle XRD patterns of the starting Fe_3O_4 NPs (a) and the Fe_3O_4NPs-UVM-7 (b). (B) Low-angle XRD pattern of the Fe_3O_4NPs-UVM-7. (C) Representative TEM image of Fe_3O_4NPs-UVM-7 with some of the magnetic nanoparticles enclosed in black circles. A higher magnification image containing a magnetite nanoparticle is shown in the inset.

nanoparticle with a size of approximately 10 nm (in good agreement with the XRD data). Nitrogen adsorption/desorption isotherms of Fe_3O_4NP-UVM-7 proved that the bimodal hierarchical porosity typical of the UVM-7 silica-based support was maintained after the incorporation of Fe_3O_4NPs (Table 1). The BET analysis found the specific surface value up to 1000 m^2/g with a mesopore volume close to 1 cm3/g and a pore diameter of 2.83 nm. Regarding the textural porosity, the most influential parameter for the PPO inhibition, the textural pore volume and the textural pore diameter were 1.6 cm3/g and 40 nm respectively. This data is in agreement with the ones found for a non-magnetized UVM-7 (Muñoz-Pina et al., 2020; Pérez-Cabero et al., 2012; Pérez-Esteve, Ruiz-Rico, Martínez-Máñez, & Barat, 2015).

Regarding the materials functionalised with thiol (-SH) and amine ($-NH_2$) groups, TGA analysis estimated an amount of organic content of 0.6 and 1.5 mmol (g SiO_2)$^{-1}$ respectively. These results fall in line with the expected degree of functionalisation reported in our previous works (Muñoz-Pina et al., 2018, Muñoz-Pina et al., 2020). The functionalisation did not modify the structure of the support as it maintains the X-ray diffraction pattern and confirmed by TEM images; however, it did affect the BET surface. In the case of Fe_3O_4NPs-UVM-7-SH, with a lower amount of -SH groups, the decrease in the specific area is less (1047 m2/g) than for Fe_3O_4NPs-UVM-7-NH_2 (496 m2/g). As the amount of organic groups on the surface increases, more mesoporous are blocked preventing nitrogen molecules from entering. Thus, both the specific surface area and the total volume of the mesopores decrease abruptly. Besides, there is a progressive reduction also in the size and volume of the intraparticle mesopore system. Nonetheless, the effect on the textural pore is much less pronounced, being sufficient for the easy diffusion of enzymes and substrate.

3.2. Apple PPO characterization and study of material/PPO ratio

The enzymatic activity of PPO in the golden delicious apple juice over time was studied. It was observed how the PPO activity (V_0) grew during the first 10 min from 45 % in recently liquefied juice until reaching its maximum activity after 10 min (100 %). Afterwards, the activity of the enzyme began to slowly decrease, reaching 75 % of the activity after 30 min under stirring. This can be explained as PPO is trapped in apple tissue plastids while polyphenols are found mainly in the vacuoles (Somboonkaew & Terry, 2011). During juice making there is a cell disruption in the apple tissue releasing the PPO and the polyphenols leading to the enzymatic browning reactions. However, a lag time period is observed before the reaction. In addition, as it is cloudy apple juice, part of the PPO which is trapped in the pulp, slowly diffuses into the medium. Considering these results, 10 min was established as the contact time between the juice and the material before removing it from the juice with a neodymium magnet.

The optimal ratio material:[PPO] was determined by testing different ratios of juice/material (Table 2). The presence of the Fe_3O_4NPs-UVM-7 did not have a significant effect on the inhibition of PPO even when using the smallest ratio juice:material. This fall in line with our previous reports when it was tested in apple juice and the enzymatic browning occurred (Muñoz-Pina et al., 2018). The support functionalised with amine groups reaches close to a 30 % of inhibition with a slight increase up to a 37 % after its removal. However, the magnetic material functionalised with -SH groups (Fe_3O_4NPs-UVM-7-SH) performed indeed a remarkable inhibition ranged from 30 to 65 % depending on the ratio. The -SH groups attached to the material surface interact with PPO so, the higher the ratio of material used the less active residual enzyme would be. In previous work, the inhibition type performed by the material no magnetic resulted in a non-competitive inhibition (Muñoz-Pina et al., 2018). This mechanism should no change as the Fe_3O_4NPs are inside the UVM-7 particles and do not interact with the PPO. Additionally, an increase of the inhibition was observed after removing the Fe_3O_4NPs-UVM-7-SH from the medium reaching similar results regardless the ratio. These results point out Fe_3O_4NPs-UVM-7-SH manages to interact and retain both, active and inhibited PPO so when the material is removed, active PPO is eliminated thus increasing the inhibition. Since the final inhibition is the same regardless of the ratio, 15 (mg/mL) was the ratio used for further analysis as well as the suggested one for the development of further industrial application for PPO inactivation purposes. Of note, this treatment could be considered a good achievement from the point of view of enzyme inactivation, although more studies should be carried out to evaluate the effect on microbiological stability.

Table 2
Inhibition (%) of the apple PPO by the Fe_3O_4NPs-UVM-7, Fe_3O_4NPs-UVM-7-SH, and Fe_3O_4NPs-UVM-7-NH_2, at pH 6.5 using catechol as substrate.

Material	Ratio [material]/juice (mg/mL)	Inhibition (%)		
		10 min	10* min	30* min
Fe_3O_4NP-UVM-7	15	0 ± 4^{aA}	2 ± 5^{aA}	5 ± 2^{aA}
	30	9 ± 5^{aA}	3 ± 5^{aA}	2 ± 6^{aA}
	60	5 ± 2^{aA}	2 ± 2^{aA}	0 ± 2^{aA}
Fe_3O_4NP-UVM-7-SH	15	33 ± 4^{cC}	68 ± 5^{aA}	59 ± 2^{bA}
	30	55 ± 4^{bB}	68 ± 7^{aA}	55 ± 6^{bA}
	60	62 ± 3^{aA}	69 ± 6^{aA}	61 ± 2^{aA}
Fe_3O_4NP-UVM-7-NH_2	15	11 ± 8^{aC}	14 ± 6^{aB}	9 ± 6^{aC}
	30	28 ± 2^{bA}	34 ± 2^{aA}	30 ± 2^{abB}
	60	23 ± 2^{bB}	37 ± 2^{aA}	35 ± 2^{aA}

10 min: determination after 10 min in agitation in the presence of the material. 10 min*: determination after 10 min in agitation and just after the remotion of the material. 30 min*: determination after 30 min in agitation just after the remotion of the material (10 min*). $^{a\text{-}c}$ Different lowercase letters indicate significant differences among times for the same material for $p < 0.05$. $^{A\text{-}C}$ Different capital letters indicate significant differences among ratios for the same material at the same time for $p < 0.05$.

Table 1
Structural properties and organic content of the Fe_3O_4NPs-UVM-7, Fe_3O_4NPs-UVM-7-SH, and Fe_3O_4NPs-UVM-7-NH_2.

Material	S_{BET}[a] (m^2/g)	Mesopore diameter (nm)[b]	Mesopore Volume (cm^3/g)[b]	Textural pore diameter (nm)[b]	Textural pore volume (cm^3/g)[b]	d_{100} (Å)[c]	2θ (°)[d]	mmol organic /g SiO_2	% Fe (wt %)
Fe_3O_4NP-UVM-7	1059	2.83	0.92	40.03	1.62	40.69	2.17	–	11.17 ± 1.7
Fe_3O_4NP-UVM-7-SH	1047	2.73	0.87	38.2	1.2	42.72	2.07	0.6	
Fe_3O_4NP-UVM-7-NH_2	496	2.49	0.3	39.3	0.87	42.72	2.07	1.5	

[a] BET specific surface calculated from the N_2 adsorption–desorption isotherms.
[b] Pore volumes and pore size (diameter) calculated from the N_2 adsorption–desorption isotherms.
[c] Diffraction peak of the reticular plane 100 calculated by $2d_{100}\,\text{sen}\theta = n\lambda$.
[d] Angle of incidence for the reflection plane.

3.3. Effect of Fe_3O_4NPs-UVM-7-SH and Fe_3O_4NPs-UVM-7-NH_2 on physical-chemical properties of the cloudy apple juice

3.3.1. Colour, pH and total soluble solids (°Brix)

Results regarding the effect of the magnetic UVM-7 functionalised with thiol and amine groups on pH, total soluble solids (TSS), and colour change are summarized in Table 3. The initial values of TSS and pH of the cloudy apple juice (12.2 °Brix and 3.99 respectively) agreed with previously reported values for the juice of the same apple variety (Sauceda-Gálvez et al., 2021). No significant changes ($p < 0.05$) in TSS were observed after the contact time and separation of the magnetic particles. No changes in the pH of the juice were observed after using non-functionalised and functionalised materials with -SH groups. In contrast, there was a significant increase in the pH (from 3.99 to 5.5) of those samples treated with Fe_3O_4NPs-UVM-7-NH_2. This rise in the pH might be not desirable as could negatively impact consumer acceptance. Similar result were found by Peña-Gómez, Ruiz-Rico, Fernández-Segovia, and Barat (2019) (Peña-Gómez et al., 2019) when using silica mesoporous microparticles to filtrate apple juice. In this case, no alteration of pH or °Brix was found when using non-functionalised silica being also stable during time. However, they found an increase in the pH of the juice when filtrated with a particle functionalised with vanillin via amine moieties. They attributed this effect to the presence of unreacted amine groups with the vanillin on the surface of the particle that leads to an increase in the pH. In the present study, the high amount of $-NH_2$ groups attached to the surface of the particles could be responsible for the observed increase of pH.

Table 3
Effect of magnetic UVM-7 materials on pH, °Brix, colour change (ΔE_{ab}*), and ascorbic acid content in apple juice at different times using 15 mg/mL of the different materials.

Sample	Time (min)	pH	Total soluble solids (°Brix)	ΔE_{ab}*	Ascorbic acid (mg/100 mL)
Control	0	3.99 ± 0.00^{b}	10.2 ± 0.0^{a}	0^{c}	22.5 ± 0.3^{a}
	10	3.99 ± 0.01^{bB}	10.2 ± 0.0^{aA}	9.24 ± 0.08^{bA}	21.0 ± 0.4^{bA}
	30	4.01 ± 0.01^{bB}	10.2 ± 0.0^{aA}	12.7 ± 0.6^{aA}	17.5 ± 1.8^{cAB}
Fe_3O_4NP-UVM-7	10	4.13 ± 0.10^{bB}	10.1 ± 0.0^{aA}	–	20.0 ± 2.0^{abA}
	10*	4.01 ± 0.08^{bB}	10.7 ± 0.1^{aA}	9.80 ± 0.08^{bA}	21.0 ± 2.0^{aAB}
	30*	4.05 ± 0.02^{bB}	10.3 ± 0.0^{aA}	13.3 ± 0.07^{aA}	17.0 ± 1.0^{bAB}
Fe_3O_4NP-UVM-7-SH	10	3.96 ± 0.03^{bB}	10.2 ± 0.0^{aA}	–	21.0 ± 2.0^{aA}
	10*	3.97 ± 0.03^{bB}	10.2 ± 0.0^{aA}	1.85 ± 0.03^{bC}	22.0 ± 2.0^{aA}
	30*	3.96 ± 0.01^{bB}	10.2 ± 0.0^{aA}	3.8 ± 0.2^{aB}	22.0 ± 2.0^{aA}
Fe_3O_4NP-UVM-7-NH_2	10	5.56 ± 0.02^{aA}	10.2 ± 0.0^{aA}	–	20.0 ± 2.0^{abA}
	10*	5.59 ± 0.02^{aA}	10.4 ± 0.1^{aA}	8.1 ± 0.3^{bB}	18.0 ± 2.0^{bB}
	30*	5.56 ± 0.01^{aA}	10.2 ± 0.0^{aA}	12.1 ± 0.6^{aA}	15.0 ± 2.0^{bB}

10 min: determination after 10 min in agitation in the presence of the material. 10 min*: determination after 10 min in agitation and just after the remotion of the material. 30 min*: determination after 30 min in agitation just after the remotion of the material (10 min*). [a-c] Different lowercase letters indicate significant differences among times for $p < 0.05$ compared with the control t = 0. [A-C] Different capital letters indicate significant differences among compounds at the same time for $p < 0.05$; in this case, both time 10 and 10* (before and after removing the material) are compared with control t = 10 min.

Concerning the influence of the magnetic mesoporous materials on the enzymatic browning, significant colour differences were recorded between the control and the samples treated with Fe_3O_4NPs-UVM-7-SH as shown in Table 3. The enzymatic browning process in absence of an inhibitor is quite fast under agitation reaching a colour difference of 9 just after 10 min, or 12 after 30 min of stirring. The same tendency is followed when the juice is treated with the non-functionalised Fe_3O_4NPs-UVM-7 and with Fe_3O_4NPs-UVM-7-NH_2 with no significant differences for $p < 0.05$. However, when the apple juice is treated with Fe_3O_4NPs-UVM-7-SH the enzymatic browning process slowed down dramatically with a colour difference of 1.8 after 10 min, 80 % less than the control. At the end of the study (30 min), even without the presence of the material in the juice, the enzymatic browning did not reach the values of the control. A value of colour change of 3.8 is achieved by the treated sample in contrast to the 12.7 of the untreated sample. It has been reported that values greater than 12 indicated absolute colour differences by the human eye, while colour changes between $3 < \Delta E_{ab}^* > 4$ only trained eye can detected (King & Derijk, 2007; Terra, Moreira, Costa, & de Morais, 2021). As said before, the double capacity of the Fe_3O_4NPs-UVM-7-SH to both inhibit and remove the PPO could explain the ability of this material to control enzymatic browning. While the material is in agitation in the apple juice, the PPO is inhibited by the thiol groups; once the material is removed, most PPO is separated from the juice. These results are in concordance with our previous works, showing that the magnetization of the UVM-7 does not affect its capacity of inhibiting the enzymatic browning in apple juice.

3.3.2. Ascorbic acid

Ascorbic acid is highly sensitive to thermal degradation during heat treatment and storage, so it is often used as a marker for product quality deterioration (Suárez-Jacobo et al., 2012). Thus, its content was also measured in the juices before and after the contact with and remotion of the materials (Table 3). The initial value of ascorbic acid found in the apple juice fall in concordance with the found in other apple juices (Xu et al., 2020) and it was observed a significant decrease after 30 min ($p < 0.05$) from 22.5 to 17.5 mg/100 mL of juice. Besides a negative correlation (see Supplementary Material, Table S1) ($r = -0.7921$, $p < 0.05$) was found between the enzymatic browning and the concentration of ascorbic acid present in the apple juice. Some authors have correlated the decrease in the vitamin with the enzymatic browning development in apples (Joshi, Rupasinghe, Pitts, & Khanizadeh, 2007; López-Nicolás, Núñez-Delicado, Sánchez-Ferrer, & García-Carmona, 2007). Ascorbic acid is oxidised to dehydroascorbic acid preventing the oxidation of other phenols present in the matrix (Arora, Sethi, Joshi, Sagar, & Sharma, 2018).

Regarding the treated juices, the presence of the Fe_3O_4NPs-UVM-7 did not change the evolution of vitamin C concentration in the juice. Amine functionalisation did not stop either the loss of vitamin C after 30 min reducing it significantly to 18 mg/100 mL. In fact, when the Fe_3O_4NPs-UVM-NH_2 was removed from the apple juice, a slight but significant decrease in the amount of vitamin C was detected. On the contrary, processing the juice with Fe_3O_4NPs-UVM-7-SH did not significantly affect the ascorbic acid content in the raw juice after 30 min.

3.3.3. Total phenolic (TPC), flavonoids, and flavonols content

A high initial value of phenolic compounds (760 ± 40 mg GAE/L) was found in the juice (Fig. 2), which is in agreement with those reported by other authors for "Golden Delicious" apple juice (Marszałek et al., 2018). The flavonoid content found in the raw juice was also high (400 ± 20 mg catechin/L) being in concordance with other studies (Abid et al., 2013). On the other hand, the flavonols content in the juice was lower compared with their analogues (98 ± 8 mg quercetin/L). Flavan-3-ols are usually the most representative phenolics in apple juice (65 %) nevertheless, flavonols are mainly found in the skin of the fruit appearing therefore in low quantities in the juice (6–15 % of total

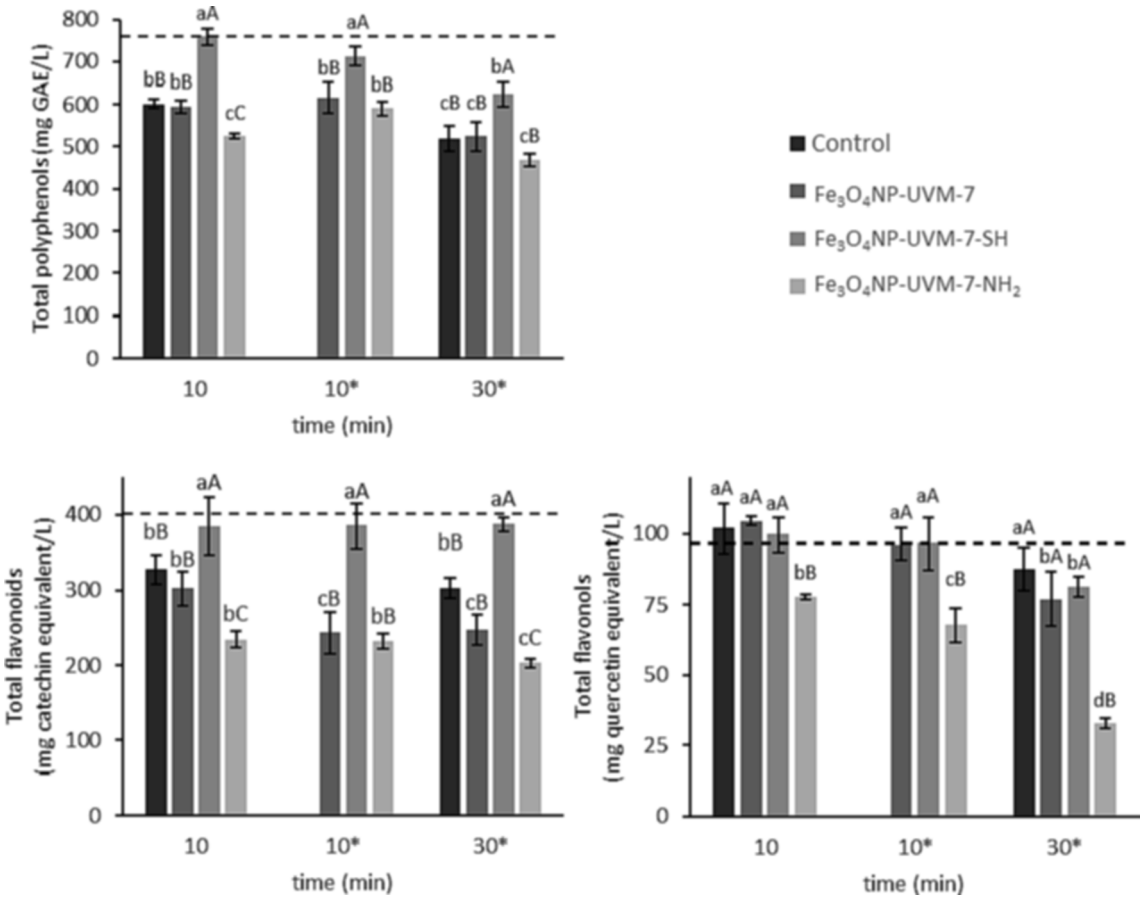

Fig. 2. Effect of the different materials on total phenolic content, flavonoids and flavonols in apple juice. Dotted line indicates the initial value in the juice at t = 0. 10 min: determination after 10 min in agitation in the presence of the material. 10 min*: determination after 10 min in agitation and just after the remotion of the material. 30 min*: determination after 30 min in agitation just after the remotion of the material (10 min*).[a-c] Different lowercase letters indicate significant differences among times for $p < 0.05$ compared with the control t = 0. [A-C] Different capital letters indicate significant differences among compounds at the same time for $p < 0.05$; in this case both time 10 and 10* (before and after removing the material) are compared with control t = 10 min.

phenolic compounds) (Fernández-Jalao, Sánchez-Moreno, & De Ancos, 2019; Massini et al., 2018).

A significant decrease (20 %) in the total content of phenolic compounds was observed in the control samples 10 min after the juice extraction, reaching a concentration close to 500 mg GAE/L after 30 min. These reductions correlated for $p < 0.05$ with the production of brown pigments and the loss of vitamin C over time (r = -0.8989 and 0.7631 respectively) (Table S1). Flavonoids were also affected by the enzymatic browning in the case of the control juice (r = -0.9438) as the initial concentration was reduced after 10 min. However, no significant changes in flavonols were found for the control over time. Similar results were obtained in the juice samples treated with Fe_3O_4NPs-UVM-7 and Fe_3O_4NPs-UVM-7-NH_2. These materials were not capable to block the oxidation of neither the phenolic compounds nor the flavonoids and flavonols. Furthermore, the UVM-7-NH_2 enhanced the loss of some phenolic (35 % loss with respect to the control), flavonoids (50 %) and flavonols (60 %) compound probably because of the pH increase. Indeed, some authors (Fu, Zhang, Wang, & Du, 2007; Liu, Han, & Ni, 2018) have shown PPO enzymatic activities in golden delicious apples rather higher at pH above 5 than close to 4.

On the other hand, the functionalised material with thiol groups was capable to stop the oxidation during the contact step and therefore the loss of the assessed bioactive compounds. Once removed from the medium, the residual enzyme did not affect the total flavonoid content, but it did affect the TPC and flavonols. It seems that the formed colour in the juice treated with -SH is mainly due to the loss of flavonols, and polyphenols according to correlations (r = −0.664, and −0.5756 for $p <$ 0.05). Noci et al. (2008) reported a 50 % of loss in the total phenolic content in apple juice after a short-time high-temperature treatment (94 °C for 26 s) and reducing the temperature to 72 °C only 10 % was recovered, still losing 40 % of TPC. So, the results with Fe_3O_4NPs-UVM-7-SH are quite promising compared to those obtained by applying thermal treatments.

3.3.4. *Total antioxidant capacity*

Antioxidant activities based on DPPH, ABTS, and FRAP revealed a significant decrease ($p < 0.05$) in the antioxidant capacity of untreated juice after 30 min (50 % for DPPH and ABTS, and 25 % for FRAP analysis) (Fig. 3). A positive correlation was found (Table S1) in the untreated juice between the three different methods (DPPH$^{\bullet}$, ABTS$^{\bullet+}$, and FRAP) for $p < 0.05$ (r > 0.9378), which is in concordance with other reported values (Fernández-Jalao et al., 2019). Besides, the generation of browning pigments in the untreated juice (ΔE_{ab}*), was also correlated with the three antioxidant capacities measured (r < -0.8722). Antioxidant capacity in the apple juice can be attributed to several antioxidants, being the contribution of polyphenols about 70–80% while vitamin C contribution is<5%. Regarding the polyphenols, the antioxidant capacity is mostly attributed to flavanols (proanthocyanidins and catechins) with a weak correlation for quercetin glycosides (flavonols) (Kolniak-Ostek et al., 2013; Massini et al., 2018). In this study, no significant correlation was found between the antioxidant activity and flavonols content, yet a significant correlation of 0.8247, 0.9071 and 0.7217 for DPPH, ABTS and FRAP respectively and the total flavonoids were found. This is in line with the analysis of total flavonoids where the

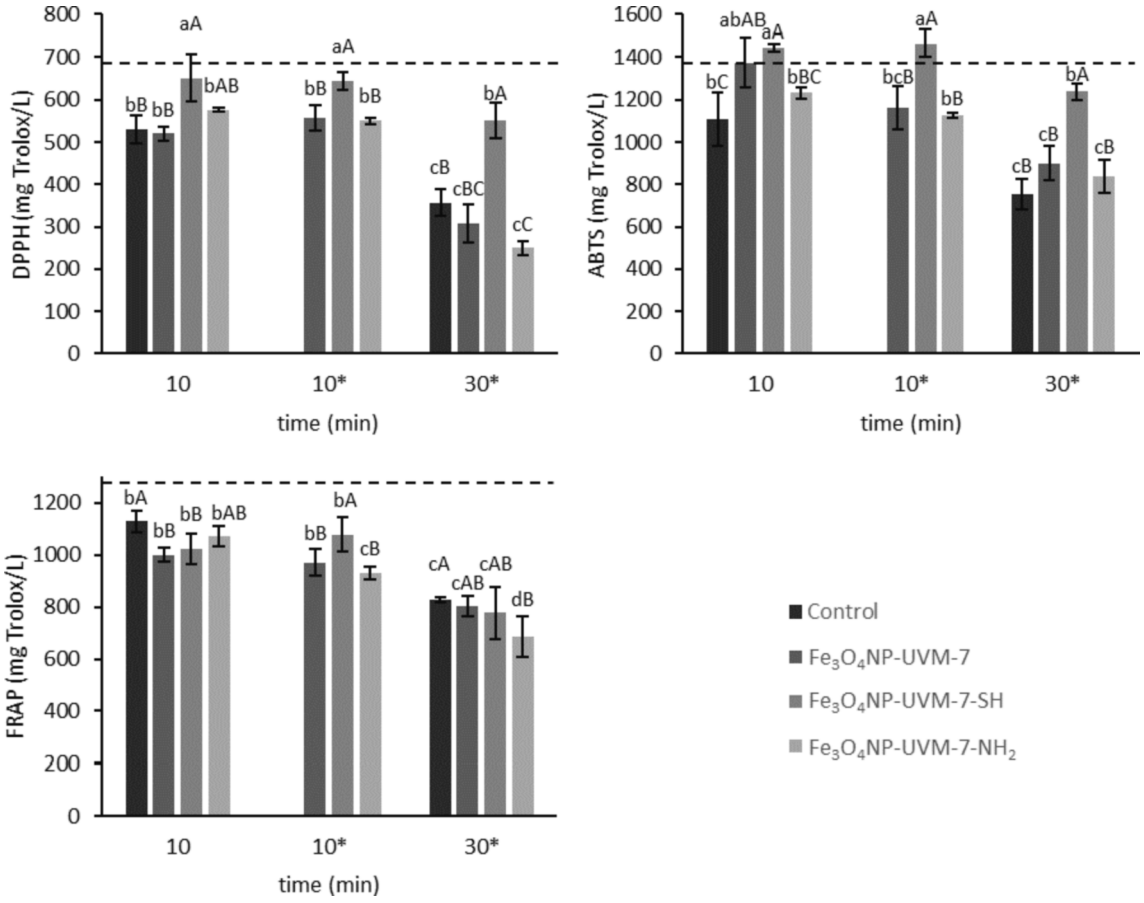

Fig. 3. Antioxidant capacity measured by three different methodologies (DPPH, ABTS, and FRAP) of cloudy apple juice. Dotted line indicates the initial value in the juice at t = 0. 10 min: determination after 10 min in agitation in the presence of the material. 10 min*: determination after 10 min in agitation and just after the remotion of the material. 30 min*: determination after 30 min in agitation just after the remotion of the material (10 min*). [a-c] Different lowercase letters indicate significant differences among times for $p < 0.05$ compared with the control t = 0. [A-C] Different capital letters indicate significant differences among compounds at the same time for $p < 0.05$; in this case both time 10 and 10* (before and after removing the material) are compared with control t = 10 min.

total flavonoid content decreased over time as does the antioxidant activity.

In agreement with the effect towards enzymatic browning, treatment with mesoporous silica materials (Fe_3O_4NPs-UVM-7 and Fe_3O_4NPs-UVM-7-NH_2) does not preserve the antioxidant activity of juices. In fact, the Fe_3O_4NPs-UVM-7-NH_2 significantly decreased the total antioxidant capacity when measured by the DPPH and ABTS method similarly as was observed for total flavonoids and flavonols.

The antioxidant capacity of juice samples treated with Fe_3O_4NPs-UVM-7-SH remained close to 1400 mg Trolox/L (in ABTS) even after it removed the medium. Only 20 % of the antioxidant activity determined by DPPH was lost after the Fe_3O_4NPs-UVM-7-SH treatment in contrast with the 50 % lost by the control. However, the antioxidant activity measured by FRAP decreased significantly to values close to the control (50 % from the initial) despite not having decreased the flavonoid content. Differences in the antioxidant activity in samples treated with Fe_3O_4NPs-UVM-7-SH depending on the analytical method could be related to the different phenolic compounds contributing to each assay. Although flavonoids are the most influential in antioxidant activity, the decrease in antioxidant capacity after treatment with Fe_3O_4NPs-UVM-7-SH measured by FRAP may be due to the loss of non-flavonoid polyphenols also present in apples. Apart from the flavonoids, some acidic phenolic compounds may influence as well to the total antioxidant capacity. In this sense, Wu et al. (2020) (Wu et al., 2020) reported that the hydroxycinnamic acid with more influence in the DPPH assay was caffeic acid, while ABTS would better correlate with ferulic acid.

As summary of the effect of the nanomaterials in the antioxidant capacity of the apple juice, we can conclude that enzymatic browning was highly related to the loss of flavonoids, vitamin C and non-flavonoid phenols, largely affecting their antioxidant power. No positive changes were found in the concentration of the bioactive compounds when treating the juice with Fe_3O_4NPs-UVM-7 and Fe_3O_4NPs-UVM-7-NH_2. On the contrary, when the juice was treated with Fe_3O_4NPs-UVM-7-SH, no loss neither in flavonoids nor vitamin C were observed. Consequently, the scarce enzymatic browning that occurs would be related to the loss of non-flavonoid polyphenols such as chlorogenic acid, caffeic acid, or ferulic acid.

4. Conclusion

A novel UVM-7 magnetic material has been prepared for the first time in order to remove it from the apple juices after treating them. The ideal percentage of magnetite in the final particle would be 11 % wt to ensure its remotion from the juice. Additionally, the results obtained after the treatment of the juice have demonstrated its potential as an anti-browning agent. For this, the optimal ratio material:[PPO] was determined as 15 mg of material per 1 mL of apple juice. Between the three materials studied (Fe_3O_4NPs-UVM-7, Fe_3O_4NPs-UVM-7-SH, and Fe_3O_4NPs-UVM-7-NH_2), the material functionalized with thiol groups is the one suitable for the inhibition of PPO, while the non-functionalized material does not cause significant changes and the support with amines has a negative influence on the juice. The enzymatic browning is reduced by 70 % when applying the material Fe_3O_4NPs-UVM-7-SH and does not affect the total content of vitamin C, flavonoids, and the

antioxidant capacity measured by ABTS. Besides, although the TPC and DPPH were still affected, the final content was higher than the control oxidized. However, more research is needed to enable scaling up the process to the industry level. In the first place, it should be analyzed the effect of the material on the major components such as proteins, fiber, or polysaccharides, as well as vitamin C and individual flavonoids and flavonols. Moreover, the material elimination through magnetic fields must be optimized in order to ensure the total recovery of the material to guarantee a safe final product, as well as to be able to reuse it for a more sustainable application.

CRediT authorship contribution statement

Sara Muñoz-Pina: Conceptualization, Methodology, Validation, Formal analysis, Investigation, Writing – original draft, Writing – review & editing, Visualization. **Aitana Duch-Calabuig:** Validation, Formal analysis, Investigation, Writing – review & editing. **Elia Ruiz De Assín David:** Validation, Investigation. **José V. Ros-Lis:** Conceptualization, Methodology, Writing – original draft, Writing – review & editing, Supervision. **Pedro Amorós:** Conceptualization, Methodology, Writing – review & editing, Supervision, Funding acquisition. **Ángel Argüelles:** Conceptualization, Methodology, Validation, Investigation, Writing – original draft, Writing – review & editing, Visualization, Supervision. **Ana Andrés:** Conceptualization, Methodology, Validation, Investigation, Writing – original draft, Writing – review & editing, Visualization, Supervision, Funding acquisition.

Declaration of Competing Interest

The authors declare that they have no known competing financial interests or personal relationships that could have appeared to influence the work reported in this paper.

Data availability

No data was used for the research described in the article.

Acknowledgement

Grant RTI2018-100910-B-C44 funded by MCIN/AEI/10.13039/501100011033 and by "ERDF A way of making Europe".

Appendix A. Supplementary data

Supplementary data to this article can be found online at https://doi.org/10.1016/j.foodres.2022.112073.

References

Abid, M., Jabbar, S., Wu, T., Hashim, M. M., Hu, B., Lei, S., Zhang, X., & Zeng, X. (2013). Effect of ultrasound on different quality parameters of apple juice. *Ultrasonics Sonochemistry, 20*(5), 1182–1187. https://doi.org/10.1016/j.ultsonch.2013.02.010

Ali, N., Popović, V., Koutchma, T., Warriner, K., & Zhu, Y. (2020). Effect of thermal, high hydrostatic pressure, and ultraviolet-C processing on the microbial inactivation, vitamins, chlorophyll, antioxidants, enzyme activity, and color of wheatgrass juice. *Journal of Food Process Engineering, 43*(1), e13036.

Ameta, S. K., Rai, A. K., Hiran, D., Ameta, R., & Ameta, S. C. (2020). Use of nanomaterials in food science. In *Biogenic Nano-Particles and their Use in Agro-ecosystems* (pp. 457–488). Springer Singapore. 10.1007/978-981-15-2985-6_24.

Aranibar, C., Pigni, N. B., Martinez, M., Aguirre, A., Ribotta, P., Wunderlin, D., & Borneo, R. (2018). Utilization of a partially-deoiled chia flour to improve the nutritional and antioxidant properties of wheat pasta. *LWT - Food Science and Technology, 89*, 381–387. https://doi.org/10.1016/j.lwt.2017.11.003

Arora, B., Sethi, S., Joshi, A., Sagar, V. R., & Sharma, R. R. (2018). Antioxidant degradation kinetics in apples. *Journal of Food Science and Technology, 55*(4), 1306–1313. https://doi.org/10.1007/s13197-018-3041-1

Bvenura, C., & Sivakumar, D. (2017). The role of wild fruits and vegetables in delivering a balanced and healthy diet. *Food Research International, 99*, 15–30. https://doi.org/10.1016/j.foodres.2017.06.046

Cappato, L. P., Ferreira, M. V. S., Guimaraes, J. T., Portela, J. B., Costa, A. L. R., Freitas, M. Q., M. Q., Cunh, R.L., Oliveira, C.A.F., Mercali, G.D., Marzack, L.D.F., &Cruz, A. G. (2017). Ohmic heating in dairy processing: Relevant aspects for safety and quality. *Trends in Food Science and Technology, 62*, 104–112. 10.1016/j.tifs.2017.01.010.

Cruz, M. G., Bastos, R., Pinto, M., Ferreira, J. M., Santos, J. F., Wessel, D. F., Coelho, E., & Coimbra, M. A. (2018). Waste mitigation: From an effluent of apple juice concentrate industry to a valuable ingredient for food and feed applications. *Journal of Cleaner Production, 193*, 652–660. https://doi.org/10.1016/j.jclepro.2018.05.109

dos Santos Aguilar, J. G., Cristianini, M., & Sato, H. H. (2018). Modification of enzymes by use of high-pressure homogenization. *Food Research International, 109*, 120–125. https://doi.org/10.1016/j.foodres.2018.04.011

El Haskouri, J., de Zarate, D. O., Guillem, C., Latorre, J., Caldes, M., Beltran, A., Beltran, D., Descalzo, A. B., Rodríguez-López, G., Martínez-Máñez, R., Marcos, M. D., & Amoros, P. (2002). Silica-based powders and monoliths with bimodal pore systems. *Chemical Communications, 4*, 330–331. https://doi.org/10.1039/B110883B

Fernández-Jalao, I., Sánchez-Moreno, C., & De Ancos, B. (2019). Effect of high-pressure processing on flavonoids, hydroxycinnamic acids, dihydrochalcones and antioxidant activity of apple 'Golden Delicious' from different geographical origin. *Innovative Food Science and Emerging Technologies, 51*, 20–31. https://doi.org/10.1016/j.ifset.2018.06.002

Fu, Y., Zhang, K., Wang, N., & Du, J. (2007). Effects of aqueous chlorine dioxide treatment on polyphenol oxidases from Golden Delicious apple. *LWT - Food Science and Technology, 40*(8), 1362–1368. https://doi.org/10.1016/j.lwt.2006.11.001

Hamad, A. F., Han, J. H., Kim, B. C., & Rather, I. A. (2018). The intertwine of nanotechnology with the food industry. *Saudi Journal of Biological Sciences, 25*(1), 27–30. https://doi.org/10.1016/j.sjbs.2017.09.004

Haskouri, J. E., Dallali, L., Fernández, L., Garro, N., Jaziri, S., Latorre, J., Guillem, C., Beltran, A., Beltran, D., & Amorós, P. (2009). ZnO nanoparticles embedded in UVM-7-like mesoporous silica materials: Synthesis and characterization. *Physica E: Low-Dimensional Systems and Nanostructures, 42*(1), 25–31. https://doi.org/10.1016/J.PHYSE.2009.08.011

Illera, A. E., Chaple, S., Sanz, M. T., Ng, S., Lu, P., Jones, J., Carey, E., & Bourke, P. (2019). Effect of cold plasma on polyphenol oxidase inactivation in cloudy apple juice and on the quality parameters of the juice during storage. *Food Chemistry: X, 3*, Article 100049. https://doi.org/10.1016/j.fochx.2019.100049

Joshi, A. P. K., Rupasinghe, H. P. V., Pitts, N. L., & Khanizadeh, S. (2007). Biochemical characterization of enzymatic browning in selected apple genotypes. *Canadian Journal of Plant Science, 87*(5), 1067–1074. https://doi.org/10.4141/CJPS07136

Jukanti, A. (2017). *Polyphenol oxidases (PPOs) in plants. Polyphenol Oxidases (PPOs) in Plants*. Springer Singapore. 10.1007/978-981-10-5747-2.

Kalinowska, M., Bielawska, A., Lewandowska-Siwkiewicz, H., Priebe, W., & Lewandowski, W. (2014). Apples: Content of phenolic compounds vs. variety, part of apple and cultivation model, extraction of phenolic compounds, biological properties. *Plant Physiology and Biochemistry, 84*. https://doi.org/10.1016/j.plaphy.2014.09.006

Kanteev, M., Goldfeder, M., & Fishman, A. (2015). Structure-function correlations in tyrosinases. *Protein Science : A Publication of the Protein Society, 24*(9), 1360–1369. https://doi.org/10.1002/pro.2734

Kaushal, N., Singh, M., & Singh-Sangwan, R. (2022). Flavonoids: Food associations, therapeutic mechanisms, metabolism and nanoformulations. *Food Research International, 157*, Article 111442. https://doi.org/10.1016/j.foodres.2022.111442

King, K. A., & Derijk, W. G. (2007). Variations of L*a*b* values among vitapan® classical shade guides: Basic science research. *Journal of Prosthodontics, 16*(5), 352–356. https://doi.org/10.1111/j.1532-849X.2007.00207.x

Kolniak-Ostek, J., Oszmiański, J., & Wojdyło, A. (2013). Effect of l-ascorbic acid addition on quality, polyphenolic compounds and antioxidant capacity of cloudy apple juices. *European Food Research and Technology, 236*(5), 777–798. https://doi.org/10.1007/s00217-013-1931-z

Kruszewski, B., Zawada, K., & Karpiński, P. (2021). Impact of high-pressure homogenization parameters on physicochemical characteristics, bioactive compounds content, and antioxidant capacity of blackcurrant juice. *Molecules, 26*(6), 1802. https://doi.org/10.3390/molecules26061802

Liu, F., Han, Q., & Ni, Y. (2018). Comparison of biochemical properties and thermal inactivation of membrane-bound polyphenol oxidase from three apple cultivars (Malus domestica Borkh). *International Journal of Food Science and Technology, 53*(4), 1005–1012. https://doi.org/10.1111/ijfs.13676

López-Nicolás, J. M., Núñez-Delicado, E., Sánchez-Ferrer, Á., & García-Carmona, F. (2007). Kinetic model of apple juice enzymatic browning in the presence of cyclodextrins: The use of maltosyl-β-cyclodextrin as secondary antioxidant. *Food Chemistry, 101*(3), 1164–1171. https://doi.org/10.1016/j.foodchem.2006.03.018

Marszałek, K., Woźniak, Ł., Barba, F. J., Skąpska, S., Lorenzo, J. M., Zambon, A., & Spilimbergo, S. (2018). Enzymatic, physicochemical, nutritional and phytochemical profile changes of apple (Golden Delicious L.) juice under supercritical carbon dioxide and long-term cold storage. *Food Chemistry, 268*, 279–286. https://doi.org/10.1016/j.foodchem.2018.06.109

Massini, L., Rico, D., & Martin-Diana, A. B. (2018). Quality Attributes of Apple Juice: Role and Effect of Phenolic Compounds. In G. Rajauria, & B. K. Tiwari (Eds.), *Fruit Juices* (pp. 45–57). Academic Press. https://doi.org/10.1016/B978-0-12-802230-6.00004-7.

Muñoz-Pina, S., Ros-Lis, J. V., Argüelles, Á., Martínez-Máñez, R., & Andrés, A. (2020). Influence of the functionalisation of mesoporous silica material UVM-7 on polyphenol oxidase enzyme capture and enzymatic browning. *Food Chemistry, 310*. https://doi.org/10.1016/j.foodchem.2019.125741

Muñoz-Pina, S., Amorós, P., Haskouri, J. E., Andrés, A., & Ros-Lis, J. V. (2020). Use of Silica Based Materials as Modulators of the Lipase Catalyzed Hydrolysis of Fats under Simulated Duodenal Conditions. *Nanomaterials, 10*(10), 1927. https://doi.org/10.3390/nano10101927

Muñoz-Pina, S., Ros-Lis, J. V., Argüelles, Á., & Andrés, A. (2019). Use of nanomaterials as alternative for controlling enzymatic browning in fruit juices. In *Nanoengineering in the Beverage Industry: Volume 20: The Science of Beverages* (pp. 163–196). Elsevier. https://doi.org/10.1016/B978-0-12-816677-2.00006-5.

Muñoz-Pina, S., Ros-Lis, J. V., Argüelles, Á., Coll, C., Martínez-Máñez, R., & Andrés, A. (2018). Full inhibition of enzymatic browning in the presence of thiol-functionalised silica nanomaterial. *Food Chemistry, 241*, 199–205. https://doi.org/10.1016/J.FOODCHEM.2017.08.059

Noci, F., Riener, J., Walkling-Ribeiro, M., Cronin, D. A., Morgan, D. J., & Lyng, J. G. (2008). Ultraviolet irradiation and pulsed electric fields (PEF) in a hurdle strategy for the preservation of fresh apple Juice. *Journal of Food Engineering, 85*(1), 141–146. https://doi.org/10.1016/j.jfoodeng.2007.07.011

Patterson, A. L. (1939). The scherrer formula for X-ray particle size determination. *Physical Review, 56*(10), 978–982. https://doi.org/10.1103/PhysRev.56.978

Peña-Gómez, N., Ruiz-Rico, M., Fernández-Segovia, I., & Barat, J. M. (2019). Study of apple juice preservation by filtration through silica microparticles functionalised with essential oil components. *Food Control, 106*, Article 106749. https://doi.org/10.1016/j.foodcont.2019.106749

Pérez-Cabero, M., Hungría, A. B., Morales, J. M., Tortajada, M., Ramón, D., Moragues, A., El Haskouri, J., Beltran, A., Beltran, D., & Amorós, P. (2012). Interconnected mesopores and high accessibility in UVM-7-like silicas. *Journal of Nanoparticle Research, 14*(8), 1–12. https://doi.org/10.1007/s11051-012-1045-8

Pérez-Esteve, É., Bernardos, A., Martinez-Manez, R., & Barat, J. M. (2013). Nanotechnology in the Development of Novel Functional Foods or their Package. An Overview Based in Patent Analysis. *Recent Patents on Food, Nutrition & Agriculture, 5*(1), 35–43. https://doi.org/10.2174/2212798411305010006

Pérez-Esteve, É., Ruiz-Rico, M., Martínez-Máñez, R., & Barat, J. M. (2015). Mesoporous Silica-Based Supports for the Controlled and Targeted Release of Bioactive Molecules in the Gastrointestinal Tract. *Journal of Food Science, 80*(11), E2504–E2516. https://doi.org/10.1111/1750-3841.13095

Putnik, P., Kresoja, Ž., Bosiljkov, T., Režek Jambrak, A., Barba, F. J., Lorenzo, J. M., … Bursać Kovačević, D. (2019). Comparing the effects of thermal and non-thermal technologies on pomegranate juice quality: A review. *Food Chemistry, 279*, 150–161. https://doi.org/10.1016/j.foodchem.2018.11.131

Raak, N., Symmank, C., Zahn, S., Aschemann-Witzel, J., & Rohm, H. (2017). Processing- and product-related causes for food waste and implications for the food supply chain. *Waste Management, 61*, 461–472. https://doi.org/10.1016/j.wasman.2016.12.027

Rascon Escajeda, L. F., Cruz Hernandez, M., Rodriguez Jasso, R. M., Charles Rodriguez, A. V., Robledo Olivo, A., Contreras Esquivel, J. C., & Belmares Cerda, R. (2018). Discussion between alternative processing and preservation technologies and their application in beverages: A review. *Journal of Food Processing and Preservation, 42*(1), e13322.

Sánchez-Cabezas, S., Montes-Robles, R., Gallo, J., Sancenón, F., & Martínez-Máñez, R. (2019). Combining magnetic hyperthermia and dual T1/T2 MR imaging using highly versatile iron oxide nanoparticles. *Dalton Transactions, 48*(12), 3883–3892. https://doi.org/10.1039/c8dt04685a

Sauceda-Gálvez, J. N., Codina-Torrella, I., Martinez-Garcia, M., Hernández-Herrero, M. M., Gervilla, R., & Roig-Sagués, A. X. (2021). Combined effects of ultra-high pressure homogenization and short-wave ultraviolet radiation on the properties of cloudy apple juice. *LWT, 136*, Article 110286. https://doi.org/10.1016/j.lwt.2020.110286

Schoeman, B. J., Sterte, J., & Otterstedt, J. E. (1995). Dynamic light scattering applied to the synthesis of colloidal zeolite. *Journal of Porous Materials, 1*(2), 185–198. https://doi.org/10.1007/BF00486657

Selimović, A., Salkić, M., & Selimović, A. (2011). Direct Spectrophotometric Determination of L-Ascorbic acid in Pharmaceutical Preparations using Sodium Oxalate as a Stabilizer. *European Journal of Scientific Research, 53*(2), 193–198.

Singh, B., Suri, K., Shevkani, K., Kaur, A., Kaur, A., & Singh, N. (2018). Enzymatic browning of fruit and vegetables: A review. In *Enzymes in Food Technology: Improvements and Innovations* (pp. 73–78). Springer Singapore. 10.1007/978-981-13-1933-4_4.

Slavin, J. L., & Lloyd, B. (2012). Health benefits of fruits and vegetables. *Advances in Nutrition, 3*(4), 506–516. https://doi.org/10.3945/an.112.002154

Somboonkaew, N., & Terry, L. A. (2011). Influence of temperature and packaging on physiological and chemical profiles of imported litchi fruit. *Food Research International, 44*(7), 1962–1969. https://doi.org/10.1016/j.foodres.2010.04.035

Suárez-Jacobo, Á., Saldo, J., Rüfer, C. E., Guamis, B., Roig-Sagués, A. X., & Gervilla, R. (2012). Aseptically packaged UHPH-Treated apple juice: Safety and quality parameters during storage. *Journal of Food Engineering, 109*(2), 291–300. https://doi.org/10.1016/j.jfoodeng.2011.09.007

Terra, A. L. M., Moreira, J. B., Costa, J. A. V., & de Morais, M. G. (2021). Development of time-pH indicator nanofibers from natural pigments: An emerging processing technology to monitor the quality of foods. *LWT, 142*, Article 111020. https://doi.org/10.1016/j.lwt.2021.111020

Thaipong, K., Boonprakob, U., Crosby, K., Cisneros-Zevallos, L., & Hawkins Byrne, D. (2006). Comparison of ABTS, DPPH, FRAP, and ORAC assays for estimating antioxidant activity from guava fruit extracts. *Journal of Food Composition and Analysis, 19*(6–7), 669–675. https://doi.org/10.1016/j.jfca.2006.01.003

Wu, C., Li, T., Qi, J., Jiang, T., Xu, H., & Lei, H. (2020). Effects of lactic acid fermentation-based biotransformation on phenolic profiles, antioxidant capacity and flavor volatiles of apple juice. *LWT, 122*, Article 109064. https://doi.org/10.1016/j.lwt.2020.109064

Xu, J., Zhou, L., Miao, J., Yu, W., Zou, L., Zhou, W., Liu, C., & Liu, W. (2020). Effect of Cinnamon Essential Oil Nanoemulsion Combined with Ascorbic Acid on Enzymatic Browning of Cloudy Apple Juice. *Food and Bioprocess Technology, 13*(5), 860–870. https://doi.org/10.1007/s11947-020-02443-8

Yamada, H., Urata, C., Aoyama, Y., Osada, S., Yamauchi, Y., & Kuroda, K. (2012). Preparation of colloidal mesoporous silica nanoparticles with different diameters and their unique degradation behavior in static aqueous systems. *Chemistry of Materials, 24*(8), 1462–1471. https://doi.org/10.1021/cm3001688